scientific reports

Check for updates

OPEN

Hair follicle transplantation promotes skin ulcer healing in a mouse model of experimental diabetes

Qian Hu[1,2], Xue Peng[1,2], Yuqian Yang[1] & Zhongshan Liu[1]✉

Chronic nonhealing wounds are complex complications of diabetes and are characterized by impaired vascular networks and persistent inflammation, making them challenging to treat. Studies have demonstrated that hair follicles possess tissue regenerative potential; however, their role in diabetic wounds remains unclear. This study aimed to investigate the impact of blood glucose levels on hair follicle activity and compare the effects of hair follicle transplantation under hyperglycemic and normoglycemic conditions on full-thickness skin wound healing in both normal and diabetic mice. The results revealed that hyperglycemia inhibited hair follicle activity. Nevertheless, hair follicle transplantation under both hyperglycemic and normoglycemic conditions promoted granulation tissue formation, collagen remodeling, and angiogenesis while reducing chronic inflammation, thereby enhancing the healing quality of diabetic wounds. Notably, hair follicles derived from normoglycemic conditions were more effective at promoting diabetic wound healing. This study provides an innovative strategy for skin regeneration in the treatment of diabetic wounds.

Keywords Diabetic wound, Hair follicles, Hair follicle stem cells, Hair follicle transplantation, Wound healing

Diabetes mellitus is a chronic metabolic disease with a continuously increasing global incidence, with type 2 diabetes mellitus (T2DM) accounting for the majority of cases. The pathophysiological features of T2DM are characterized primarily by insulin resistance and insufficient insulin secretion, resulting in sustained hyperglycemia. Long-term hyperglycemia can lead to a variety of complications, among which diabetic foot is particularly prominent. Globally, approximately 18.6 million people suffer from diabetic foot ulcers each year. In diabetic patients, nearly 80% of lower limb amputations are preceded by ulcer formation, and this condition is closely associated with an increased risk of mortality. It is estimated that 50–60% of diabetic foot ulcers are infected, and approximately 20% of moderate to severe infections may result in lower limb amputation. The five-year mortality rate for patients with diabetic foot is approximately 30%, increasing to as high as 70% for those who undergo major amputations, severely impacting patients' quality of life[1]. Delayed wound healing in diabetic patients is attributed to multiple factors, including hyperglycemia, neuropathy, microvascular complications, chronic inflammation, and impaired immune function. These conditions synergistically contribute to slow and complicated wound repair[2]. Currently, conventional treatments—such as debridement, infection control, negative-pressure wound therapy, and autologous skin grafting—have shown limited efficacy in certain cases. Moreover, these approaches are often associated with high costs and difficulties in reconstructing skin appendages[3].

Regenerative medicine has brought new hope to the treatment of diabetic wounds. As an emerging technique in this field, hair follicle (HF) transplantation offers unique advantages. HFs are the only skin appendages with cyclical regenerative capacity. HF transplantation causes minimal damage to the donor site, is easy to perform, and requires simple postoperative care. Compared with traditional scar repair methods, this method also results in better wound healing and improved tissue quality[4–6]. Studies have shown that HF transplantation promotes wound healing and reduces scar formation. Hair follicle stem cells (HFSCs) play a key role in this process by differentiating into epithelial cells and accelerating wound coverage. Clinically, wounds treated with HF transplantation demonstrate better resistance to friction, enhanced flexibility, and smoother tissue appearance. This technique is also associated with fewer complications and improved quality of life[6]. Although

[1]Department of Plastic and Burns, The Affiliated Hospital of Guizhou Medical University, Guizhou, People's Republic of China. [2]Qian Hu and Xue Peng contributed equally to this work. ✉email: 179417304@qq.com

HF transplantation has been applied successfully in chronic lower limb wounds, challenges remain in diabetic wounds due to the high-glucose environment, which may impair HF viability and reduce treatment efficacy[7]. In diabetic foot ulcers, the scarcity and fragility of lower limb HFs further hinder healing[4]. Despite this, HF transplantation is considered to have strong therapeutic potential for chronic diabetic wounds. Research suggests that HFs contribute to wound healing by promoting keratinocyte proliferation, reducing inflammation, enhancing angiogenesis, and accelerating extracellular matrix (ECM) deposition[8–12]. HFSCs, as multipotent stem cells, are especially important—they can differentiate into endothelial cells and promote neovascularization. Additionally, HFs regulate fibroblast function and epithelialization, creating a more favorable wound-healing environment[13–15]. For example, Ansell et al.[14] reported that anagen-phase HFs enhanced re-epithelialization in mouse wounds by promoting keratinocyte proliferation, reducing inflammatory infiltration, increasing angiogenesis, and accelerating ECM deposition. Lough et al.[6] reported that transplanting HFSCs via hydrogel scaffolds enhanced epithelialization, hair regeneration, and angiogenesis. However, studies on HF viability and efficacy under hyperglycemic conditions are limited. High glucose may impair HFs through a reduced blood supply or suppressed stem cell activity[16]. Since HF viability is key to transplantation success[17], understanding HF function under diabetic conditions is critical. This study aimed to explore the role of HF transplantation in diabetic wound healing and evaluate the impact of hyperglycemia on HF activity. We hypothesize that HFs retain their viability and differentiation potential in a high-glucose environment and can continue to promote wound repair. To test this hypothesis, autologous or syngeneic HFs were transplanted into full-thickness skin wounds in both normoglycemic and streptozotocin-induced diabetic mice. We assessed HF activity under hyperglycemic conditions and examined wound healing outcomes, including angiogenesis, cell proliferation, granulation tissue formation, and other key indicators. This research aims to provide an innovative and effective strategy for diabetic wound treatment.

Results

We conducted the experiment according to the following procedures (Fig. 1a). To verify the successful establishment of the experimental diabetic mouse model, we assessed several parameters, including body weight changes, fasting blood glucose levels, glucose tolerance, histological changes in the liver, and microcirculatory alterations at the dorsal wound site.

Body weight changes

Body weight was recorded at weeks 0, 2, 4, 6, 8, 10, and 12 for the mice fed either a normal diet or a high-fat, high-sugar (HFHS) diet (Fig. 1b). The body weight of the mice in the HFHS group gradually increased during the early phase of the experiment. Starting at week 4, their body weight was greater than that of the normal diet (NG) group ($P<0.05$). Two weeks after streptozotocin (STZ) injection, body weight began to decline and was lower than that of the NG group by week 9 ($P<0.05$), indicating that metabolic disturbances are consistent with diabetic progression.

Fasting blood glucose and glucose tolerance

Fasting blood glucose levels were recorded from weeks 7 to 12 (Fig. 1c). Compared with that in the normal control (NC) group, fasting blood glucose was elevated in the diabetic wound (DW), DW + HF(NG), and DW + HF(HG) groups ($P<0.05$). To further assess glucose metabolism, an intraperitoneal glucose tolerance test (GTT) was performed at week 9 (four weeks after STZ injection) (Fig. 1d). At 0, 30, 60, and 120 min, blood glucose levels in the DW, DW + HF(NG), and DW + HF(HG) groups were consistently higher than those in the NC, NC + HF(NG), and NC + HF(HG) groups. The corresponding area under the curve (AUC) values were also elevated ($P<0.05$) (Fig.1e), indicating impaired glucose tolerance.

Liver histopathology

Histological evaluation of liver tissues via H&E staining was performed at week 9 (Fig. 1f). In the NG group, the liver cords were clearly and regularly arranged, and the hepatocyte nuclei appeared normal. In contrast, the HG group presented disorganized hepatic cords, enlarged hepatocytes, and numerous intracellular lipid vacuoles and fat droplets, indicating the presence of hyperlipidemia and fatty liver.

Ultrastructural changes in the microvasculature of diabetic mice

Four weeks after STZ injection, transmission electron microscopy (TEM) was used to observe the ultrastructure of the dorsal skin microvasculature in the mice (Fig. 2a). In the NG group, the vascular lumens appeared normal, the endothelial cells showed no protrusions, and the mitochondria were short rod- or spheroid-shaped with uniform electron density and an intact structure, without swelling, vacuolization, or crista disruption. In contrast, the HG group exhibited localized and diffuse thickening of the capillary basement membrane. Endothelial cells proliferate and form hump-like, papillary, or bridge-like structures that cross the vascular lumen. In addition, the mitochondria were enlarged and showed uneven electron density, and some exhibited swelling, rupture, reduced matrix density, and transparency, with autophagosomes also observed. These changes are key indicators of microcirculatory dysfunction. Quantitative analysis revealed that the endothelial cell thickness in the HG group was greater than that in the NG group ($P<0.05$) (Fig. 2b).

Changes in hair follicle activity in diabetic mice

To investigate the impact of hyperglycemia on hair follicle activity, hair follicles were collected four weeks after STZ injection, and alkaline phosphatase (ALP) activity in follicular tissue was assessed (Fig. 2c). ALP is a critical marker of hair follicle activity in both humans and mice and is considered one of the most prominent indicators

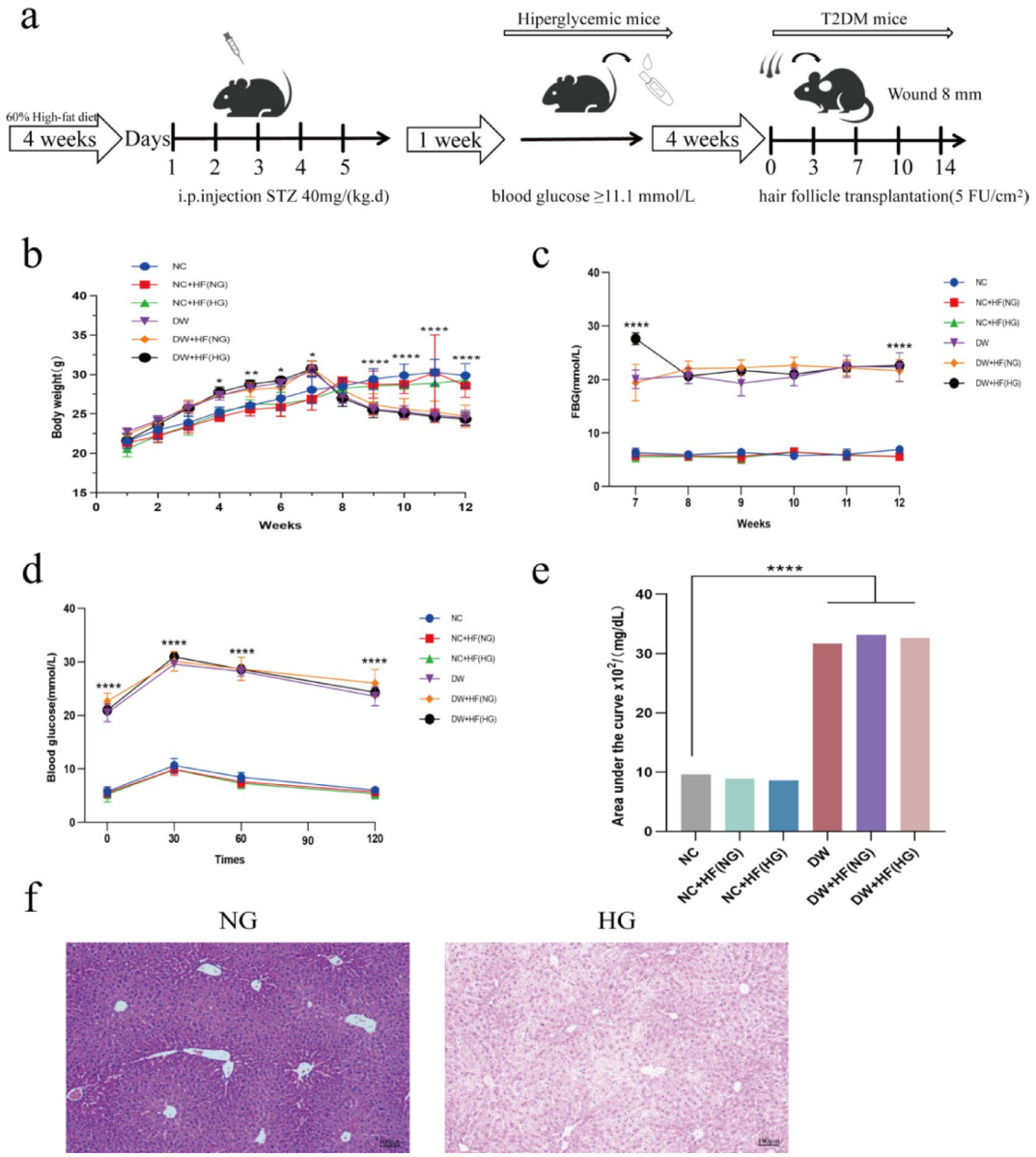

Fig. 1. Establishment of a Diabetic Wound Model in Mice and Evaluation of Hair Follicle Transplantation for Promotion of Diabetic Wound Healing. (**a**) Experimental workflow diagram. (**b**) Changes in mouse body weight. (**c**) Fasting blood glucose (FBG) measurements. (**d**) Oral glucose tolerance test (OGTT) results. (**e**) Data from (**d**), area under the glucose tolerance curve (AUC) for the OGTT results. (**f**) Pathological changes in the livers of the NG and HG groups, as shown by H&E staining. The error bars represent the means ± standard deviations (SDs), $n = 6$ per group. Statistical analysis was performed via one-way ANOVA. with p values denoted as $^{*}P < 0.05$, $^{**}P < 0.01$, $^{****}P < 0.0001$.

of follicular viability[18]. The results revealed that ALP activity in the HG group was lower than that in the NG group ($P < 0.05$), suggesting that hyperglycemia markedly suppresses hair follicle activity.

Hair follicle transplantation promotes wound re-epithelialization

The effect of hair follicle transplantation on wound healing was observed and statistically analyzed (Fig. 3a、b). On day 3, the wound healing rate in the NC group was 38.80%, that in the NC + HF(NG) group was 57.00%, which was significantly greater than that in the NC group ($P < 0.05$). The healing rate in the NC + HF(HG) group was 50.04%, which was also significantly greater than that in the NC group ($P < 0.05$). The healing rate in the DW group was 27.07%, which was significantly lower than that in the NC group and lower than that in both the NC + HF(NG) and NC + HF(HG) groups ($P < 0.05$). The healing rate in the DW + HF(NG) group was 49.66%, which was significantly greater than that in the DW group ($P < 0.05$), and in the DW + HF(HG) group, it was 46.99%, which was also significantly greater than that in the DW group ($P < 0.05$). These findings indicate that hair follicle transplantation promotes wound healing in both normal and high-glucose environments. On

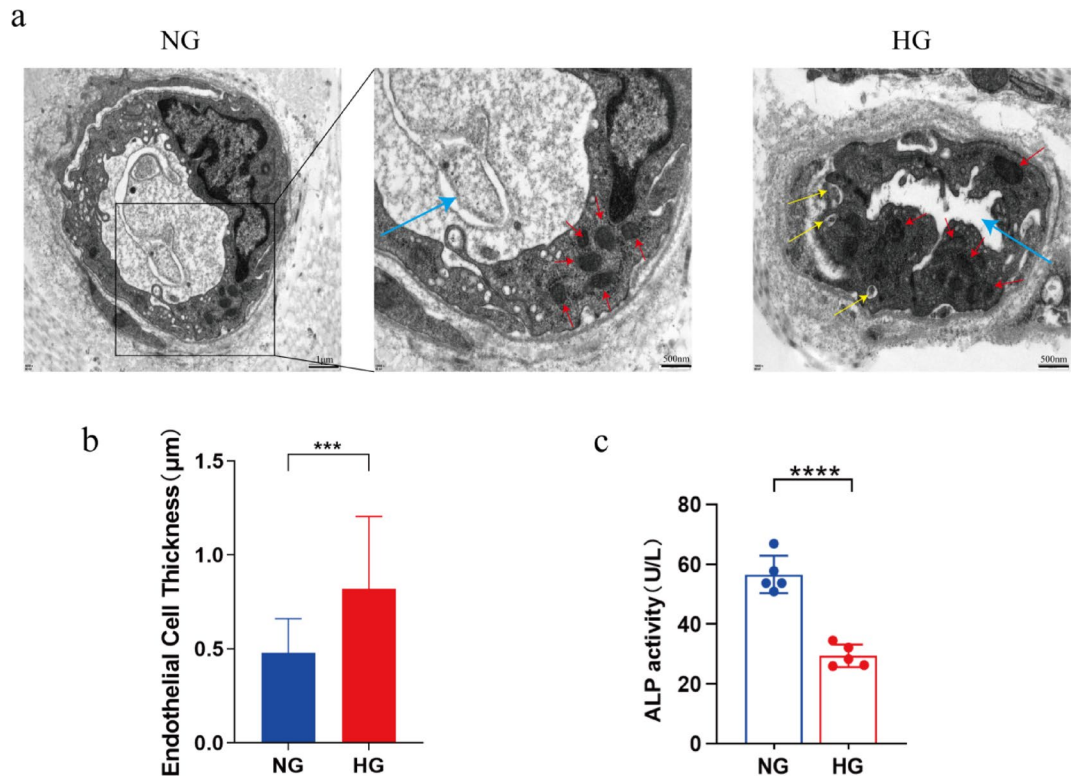

Fig. 2. Changes in Microcirculation and Hair Follicle Activity in Diabetic Mice. (**a**) Transmission electron microscopy (TEM) images showing ultrastructural changes in microvessels under different glycemic conditions in the NG and HG groups. Red arrows indicate mitochondria; blue arrows indicate the vascular lumen; yellow arrows indicate autophagosomes. (**b**) The thickness of endothelial cells in the NG and HG groups as determined via TEM. (**c**) Statistical analysis of alkaline phosphatase (ALP) activity in the NC and HG groups. All the data are presented as the means ± standard deviations (SDs), $n = 6$ per group. The error bars represent the means ± SDs. Statistical analysis was performed via independent t tests, with p values denoted as *** $P < 0.001$ and **** $P < 0.0001$.

day 7 after surgery, the healing rate in the NC + HF(NG) group was 89.23%, which was significantly greater than that in the NC group (77.54%). The healing rate in the NC + HF(HG) group was 86.67%, which was not significantly different from that in the NC group ($P > 0.05$). The healing rate in the DW group was 45.68%, that in the DW + HF(NG) group was 85.93%, and that in the DW + HF(HG) group was 75.43%. Both the DW + HF(NG) and DW + HF(HG) groups had significantly higher healing rates than did the DW group ($P < 0.05$). The difference in healing rates between the NC + HF(NG) and NC + HF(HG) groups was significant ($P < 0.05$), suggesting that the effect of hair follicle transplantation is weaker under high-glucose conditions. On day 10 after surgery, the healing rate in the NC + HF(NG) group was 91.46%, which was significantly greater than that in the NC group (91.46%). The healing rate in the NC + HF(HG) group was 95.63%, with no significant difference ($P > 0.05$). The healing rate in the DW group was 74.79%, which was significantly lower than that in the other groups ($P < 0.05$). The healing rate in the DW + HF(NG) group was 98.46%, and that in the DW + HF(HG) group was 96.47%, both of which were significantly greater than that in the DW group ($P < 0.05$). The healing rate in the NC + HF(NG) group was significantly greater than that in the DW + HF(HG) group ($P < 0.05$). Hair follicle transplantation from normal blood glucose environments appears to have a better effect, possibly because of the sustained action of hair follicles and their immune privilege characteristics. On day 14 after surgery, all groups except the DW group had complete wound closure, with significantly lighter scars after hair follicle transplantation. Overall, hair follicle transplantation promoted diabetic wound healing and improved healing quality.

Hair follicle transplantation promotes epidermal restoration and collagen deposition

Hematoxylin and eosin (H&E) staining (Fig. 4a) revealed the formation of an epidermal cell layer in the wound area. In the NC group, wound healing occurred primarily through tissue contraction, with evenly distributed hair follicles surrounding the wound. The regenerated epidermis appeared thin, with relatively few newly formed hair follicles and blood vessels. In contrast, the DW group presented large epidermal defects and incomplete wound closure. Compared with the NC group, both the NC + HF (NG) and NC + HF (HG) groups presented clearly stratified skin architecture, including visible hair follicles and sebaceous glands. The epidermis was significantly thickened. Similarly, in comparison with the DW group, the DW + HF (NG) and DW + HF (HG) groups also presented epidermal thickening. (Fig. 4d) Notably, the DW + HF (NG) group demonstrated increased numbers of hair follicles and newly formed blood vessels, whereas these features were less prominent in the DW + HF

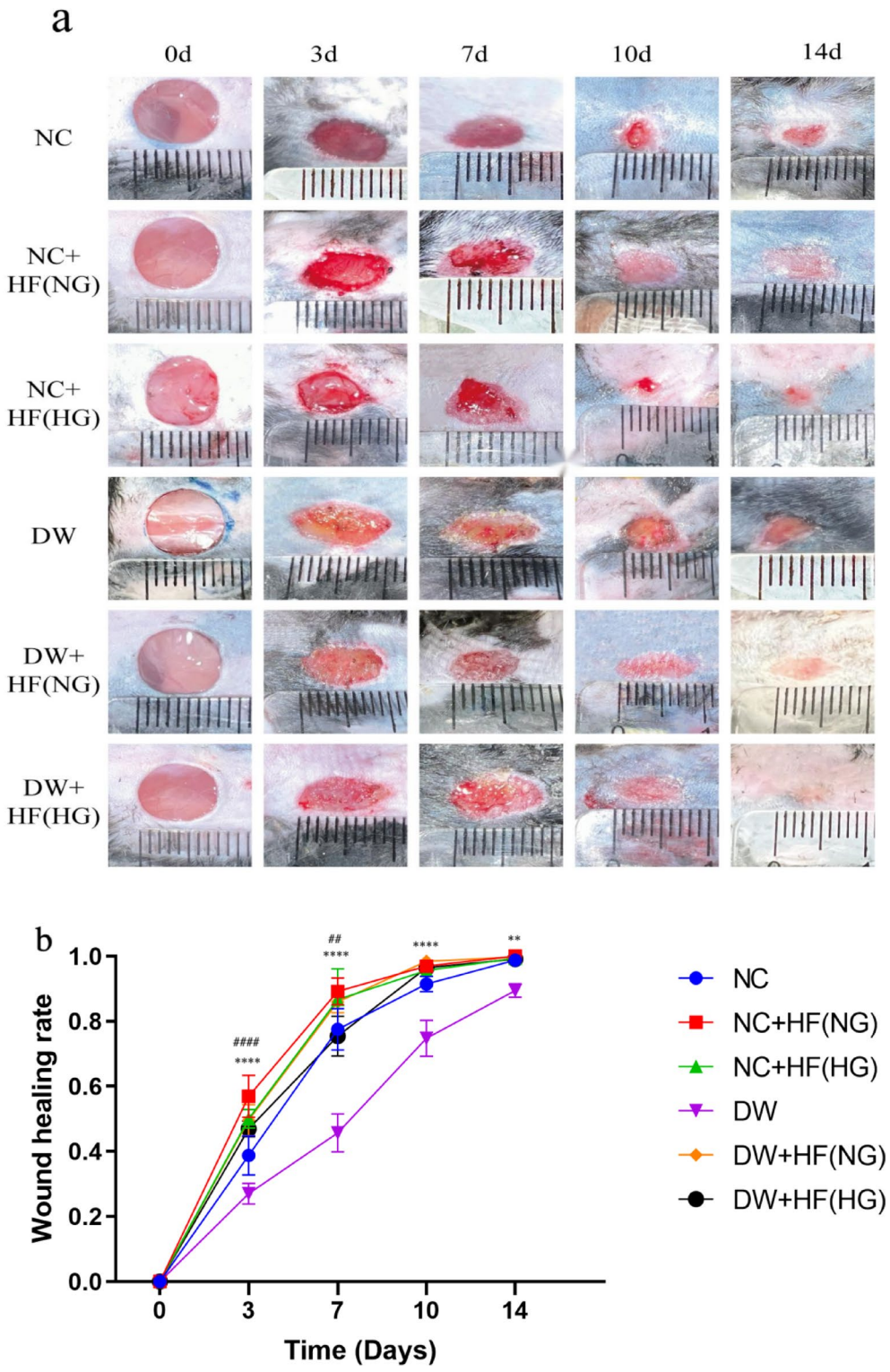

Fig. 3. Wound Healing Assessment After Hair Follicle Transplantation on STZ-Induced Diabetic Wounds. (a) Representative images of wounded skin on days 0, 3, 7, 10, and 14 posttransplantation, showing wound healing progression. (b) The wound healing rate of each group was analyzed on days 0, 3, 7, 10, and 14 after transplantation. The error bars represent the means ± SDs. Statistical analysis was performed via two-way ANOVA. Compared with the NC+HF(NG) group and the NC+HF(HG) group, the NC+HF(NG) group and the NC+HF(HG) group were significantly different on days 3 and 7 ($^{\#\#\#\#}$ $p < 0.0001$, $^{\#\#}$ $p < 0.01$). Compared with the DW+HF(NG) group and DW+HF(HG) group, the DW+HF(NG) group and DW+HF(HG) group presented statistically significant differences on days 3, 7, 10, and 14 (** $P < 0.05$, **** $P < 0.0001$).

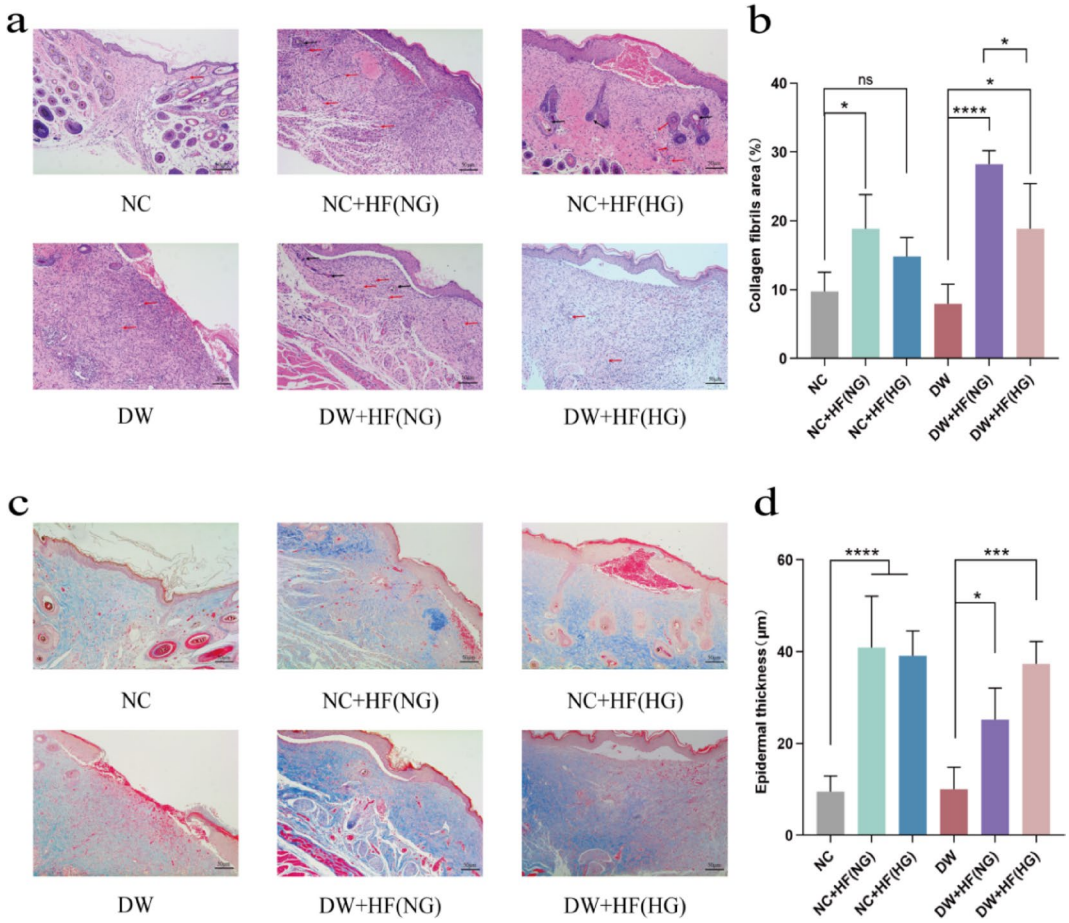

Fig. 4. Histological and mass assessment of granulation tissue and collagen deposition.(**a**) HE staining was used to examine granulation tissue in different treatment groups; scale bar, 50 μm; black arrows indicate hair follicle cells; red arrows indicate new blood vessels; (**b**) collagen was stained via Masson's trichrome; (**c**) collagen deposition and tissue fibrosis were assessed via Masson's trichrome staining. Scale bar, 50 μm. (**d**) Epidermal thickness on day 14 after transplantation. The error bars represent the means ± SDs. Statistical analysis was performed via one-way ANOVA. * $P < 0.05$, *** $P < 0.001$, **** $P < 0.0001$, $^{ns}P > 0.05$.

(HG) group. Masson's trichrome staining (Fig. 4c) revealed that, compared with the NC group, the NC + HF (NG) group presented significantly more organized collagen fibers, greater collagen deposition, and an increased amount of collagen fibers on postoperative day 14 ($P < 0.05$). In contrast, the NC + HF (HG) group presented limited collagen deposition, with no statistically significant difference compared with the NC group ($P > 0.05$). Compared with the DW group, both the DW + HF (NG) and DW + HF (HG) groups presented more orderly collagen fiber arrangements and increased collagen content on day 14. Among them, the DW + HF (NG) group presented significantly greater collagen deposition and more organized collagen fibers ($P < 0.05$). (Fig. 4b)

Summary: On day 14 after hair follicle transplantation, the wound surface exhibited an epidermal layer centered around the transplanted follicles. The transplanted follicles gradually integrated with the surrounding tissue. In the DW group, the wound bed was predominantly filled with granulation tissue and covered by a scab, with no formation of an epidermal layer. Hair follicle transplantation effectively promoted the formation of skin appendages, epidermal thickening, and increased collagen deposition and fiber organization.

Hair follicle transplantation promotes granulation tissue formation

Hair follicle transplantation not only promoted granulation tissue formation but also improved the inflammatory state of the wound. Ki67 is a well-established marker of cellular proliferation that is expressed exclusively in actively cycling cells and is absent in quiescent cells[19]. To investigate the effects of normal and high-glucose-conditioned hair follicles on cell proliferation within granulation tissue, Ki67 immunofluorescence staining was performed. Compared with that in the NC and DW groups, the expression of Ki67 was significantly increased in all hair follicle transplantation groups (NC + HF (NG), NC + HF (HG), DW + HF (NG), and DW + HF (HG)), indicating enhanced cellular proliferation following hair follicle transplantation (Fig. 5). Among these groups, the DW + HF (NG) group presented the highest level of Ki67 expression, further confirming the prominent role of normal hair follicles in promoting cell proliferation in the diabetic wound model.

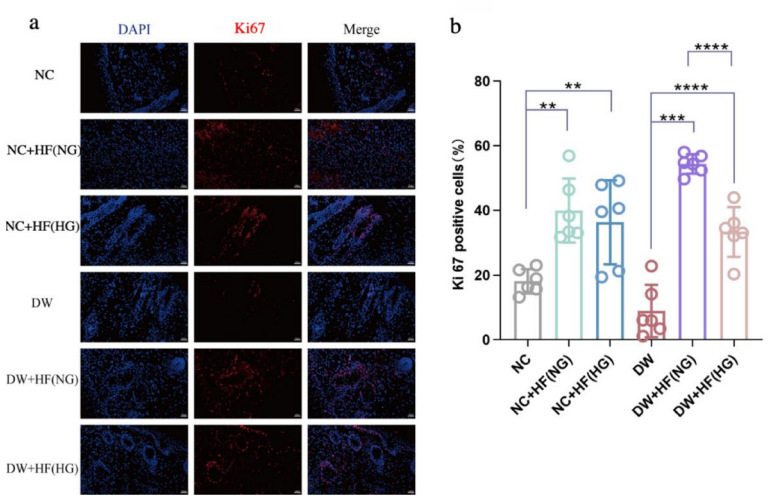

Fig. 5. Evaluation of Cellular Proliferation in Wounds via Ki67 Immunofluorescence. (**a**) Representative immunofluorescence images of Ki67 staining (red) in skin tissues from each group on day 14 posttreatment, with DAPI (blue) used for nuclear counterstaining. Scale bar: 50 μm. (**b**) Quantitative analysis of Ki-67 fluorescence intensity. The error bars represent the means ± SDs. Statistical analysis was performed via one-way ANOVA. with p values denoted as $^{**}P < 0.01$, $^{***}P < 0.001$,$^{****}P < 0.0001$.

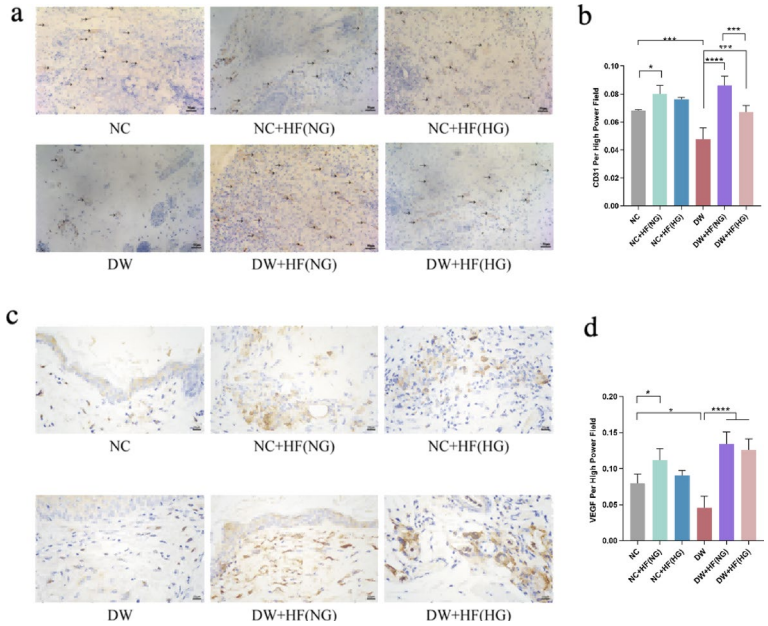

Fig. 6. Representative images of immunohistochemical staining for CD31 and VEGF in wound tissues.(**a**) Representative images of CD31 immunohistochemical staining of wound tissues from each group. Scale bars: 50 μm. (**b**) Representative images of VEGF immunohistochemical staining of wound tissues from each group. Scale bars: 20 μm. (**c**) Quantitative analysis of CD31-positive staining in wound tissues. (**d**) Quantitative analysis of VEGF-positive staining in wound tissues. All data are presented as the means ± standard deviations (SDs), n = 6 per group. Statistical analysis was performed via one-way ANOVA, with p values denoted as $^{ns}P > 0.05$, $^{*}P < 0.05$, $^{***}P < 0.001$, and $^{****}P < 0.0001$.

Hair follicle transplantation promotes angiogenesis

Effective microcirculation is closely associated with improved wound healing[20]. On day 14, CD31 immunohistochemistry was performed to evaluate and quantify the microvessel density at the wound sites. CD31 is a well-established marker of endothelial cells[21] and is commonly used in immunohistochemical staining to assess the degree of tissue vascularization. As shown in the CD31-stained images (Fig. 6), hair follicle transplantation markedly increased the microvessel density within the wound area. The percentage of CD31-positive cells in the NC + HF (NG) group was significantly greater than that in the NC group ($P < 0.05$).

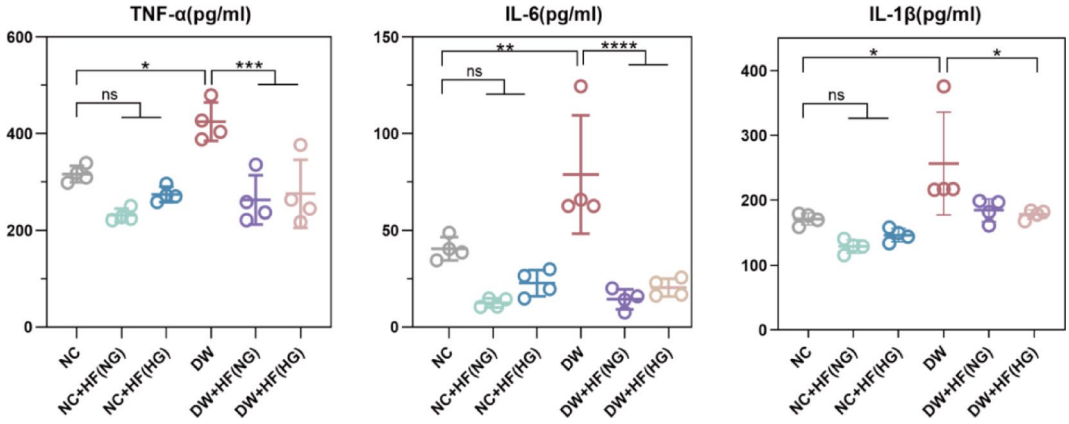

Fig. 7. Quantitative Analysis of Skin Inflammatory Markers (TNF-α, IL-6, and IL-1β) in Each Group. The levels of the inflammatory markers TNF-α, IL-6, and IL-1β were quantified across groups. All data are presented as the means ± standard deviations (SDs), n = 6 per group. Statistical analysis was performed via one-way ANOVA, with p values denoted as $^{ns}P > 0.05$, $^{*}P \leq 0.05$, $^{***}P < 0.001$, and $^{****}P < 0.0001$

Although the NC + HF (HG) group showed a slight increase, it was not significantly different from the NC group. In contrast, both the DW + HF (NG) and DW + HF (HG) groups presented significantly greater CD31-positive rates than did the DW group ($P < 0.05$), with the DW + HF (NG) group showing the greatest microvessel density. Moreover, the microvessel density in the DW + HF (NG) group was significantly greater than that in the DW + HF (HG) group. Vascular endothelial growth factor (VEGF)[22], a key protein in angiogenesis, belongs to a family of growth factors essential for neovascularization during wound healing. As shown in Fig. 6, VEGF expression was significantly greater in the NC + HF (NG) group than in the NC group ($P < 0.05$) on day 14 after hair follicle transplantation. However, the NC + HF (HG) group was not significantly different from the NC group ($P > 0.05$). Both the DW + HF (NG) and DW + HF (HG) groups presented significantly higher VEGF expression than the DW group did ($P < 0.05$).

Anti-inflammatory effects of hair follicle transplantation

One of the primary reasons for impaired wound healing in diabetes patients is the prolonged proinflammatory phase. A high-glucose environment promotes the inflammatory response by upregulating the expression of proinflammatory cytokines, such as TNF-α, IL-1β, and IL-6, and impairs the function of vascular endothelial cells, thereby further delaying wound healing[23–24]. In this study, we assessed the levels of inflammatory cytokines in skin tissue on day 14 following hair follicle transplantation (Fig. 7). The results revealed that both TNF-α and IL-6 levels were significantly reduced in the DW + HF (NG) and DW + HF (HG) groups ($P < 0.05$), whereas IL-1β levels were increased in the DW + HF (HG) group ($P < 0.05$). These findings indicate that hair follicle transplantation can effectively suppress inflammation induced by a hyperglycemic environment and alleviate wound inflammation. In contrast, although the cytokine levels in the NC + HF (NG) and NC + HF (HG) groups tended to decrease compared with those in the NC group, the differences were not statistically significant ($P > 0.05$).

Materials and methods

Ethics statement

Specific pathogen-free (SPF)-grade male C57BL/6 mice were purchased from Beijing Vital River Laboratory Animal Technology Co., Ltd. (production license number: SCXK (Jing) 2021-0006; quality certificate number: NO.110011241100619078). All animals were housed under standard barrier conditions at Guizhou Medical University. The study was approved by the Animal Ethics Committee of Guizhou Medical University (Approval No. N 2305133). All procedures were conducted in accordance with the guidelines provided by the Institute of Laboratory Animal Resources for the Care and Use of Laboratory Animals and in compliance with the ARRIVE guidelines.

Diabetic wound model

A total of 36 male SPF-grade C57BL/6 mice (18–22 g, approximately 6 weeks old) were housed at 24 °C ± 1 °C and 55% ± 5% humidity with a 12-hour light/dark cycle. Food and water were provided ad libitum. The mice were weighed to 1 g accuracy and randomly divided into two groups: normal glucose (NG, $n = 18$) and high glucose (HG, $n = 18$). The NG group received a standard diet, whereas the HG group was fed a high-fat diet that provided 60% of the calories from fat (commercial diet D12492). Body weight was monitored regularly, and mice whose body weights were below the standard threshold were excluded. The inclusion criterion for HG-treated mice was a body weight equal to or greater than that of the NG-treated mice. After 4 weeks, HG mice that met the weight criteria were intraperitoneally injected with streptozotocin (STZ, 40 mg/kg; Solarbio, China) for 5 consecutive days to establish diabetic mice[25]. The control animals received intraperitoneal injections of citrate buffer (pH 4.5). Blood glucose levels were measured one week later via a glucometer. Mice with nonfasting blood

glucose levels > 200 mg/dL (11.1 mmol/L) were maintained for an additional 4 weeks before full-thickness skin wounds were created[26]. After 4 weeks, 18 NG-fed mice were randomly divided into three groups ($n = 6$/group): the normal control group (NC), the NC plus HFs under normal glucose conditions group (NC + HF(NG)), and the NC plus HFs under high glucose conditions group (NC + HF(HG)). Similarly, 18 HG-treated mice with blood glucose levels > 16.67 mmol/L were randomly divided into three groups ($n = 6$/group): the diabetic wound group (DW), the DW plus hair follicles under normal glucose conditions group (DW + HF(NG)), and the DW plus hair follicles under high glucose conditions group (DW + HF(HG)).

Surgical procedure

Acquisition of whisker hair follicles

The surgical site was disinfected with ultraviolet light for 30 min. The mice were weighed and then anesthetized via intraperitoneal injection of Nembutal (35 mg/kg, Sigma, USA). After successful anesthesia, the mice were placed on the operating table. The whisker area was disinfected with iodine three times. A wedge-shaped skin sample (0.4–0.5 cm × 0.2–0.3 cm) was carefully excised from the whisker pad on one side of the mouse, along the direction of hair follicle growth, reaching the hair follicle base while ensuring the preservation of the hair follicle structure. Hemostasis was achieved at the excision site, and interrupted sutures were applied via absorbable methods. The skin sample was immersed in Ringer's solution, and after disinfection, it was placed on a microscopic operating stage. After being rinsed three times with saline, whisker hair follicles were carefully separated from the skin sample via microscopic instruments. The lower part of the hair follicle was gently squeezed, revealing the hair papilla with a red blood supply. The surrounding tissue enveloping the hair follicle was trimmed, and the hair papilla was removed or the hair shaft was extracted as per the specific group treatments. The hair follicles were placed in a sterile culture dish containing culture medium and kept on ice if the temperature was too high.

Whisker hair follicle skin graft

The skin on the posterior midline of the back was shaved using a hair clipper. The mouse's body was sprayed with 75% alcohol for disinfection. Afterward, iodine tincture was applied three times to disinfect the surgical site, and sterile drapes were placed. Whisker hair follicles from different types of mice were acquired via the method described above. The following treatments were applied to the groups:

1. Normal Blood Glucose Mouse Wound Group (Normal Control Group, NC group): PBS was applied to the wounds of normal mice.
2. Normal Blood Glucose Mouse Wound Normal Blood Glucose Hair Follicle Grafting Group (NC plus HFs under normal glucose conditions, NC + HF(NG) group): Autologous hair follicles were transplanted into the wounds of normal mice.
3. Normal Blood Glucose Mouse Wound High-Glucose Hair Follicle Grafting Group (NC plus HFs under high-glucose conditions, NC + HF(HG) group): Syngeneic high-glucose hair follicles were transplanted into the wounds of normal mice.
4. Diabetic Mouse Wound Group (Diabetic Wound, DW group): PBS was applied to the wounds of diabetic mice.
5. Diabetic Mouse Wound Normal Blood Glucose Hair Follicle Grafting Group (DW plus hair follicles under normal glucose conditions, DW + HF(NG) group): Syngeneic normal blood glucose hair follicles were transplanted into the wounds of diabetic mice.
6. Diabetic Mouse Wound Autologous High-Glucose Hair Follicle Grafting Group (DW plus hair follicles under high-glucose conditions, DW + HF(HG) group): Autologous high-glucose hair follicles were transplanted into the wounds of diabetic mice.

The surgical site was located on the dorsal midline of the mouse, and the skin was shaved. A circular wound was created by marking a 0.8 cm diameter incision on the designated skin area. After disinfection and draping, the full-thickness skin was excised along the marked line, with careful attention to hemostasis. Hair follicle grafting (autologous or syngeneic) was performed at a density of 5FU/cm^2[17]. The wound was covered with petroleum jelly gauze and clean gauze, and the area was finally secured with an elastic bandage. The wound healing process was observed on days 0, 3, 7, 10, and 14, and images were collected for analysis. The wound healing rate was calculated via ImageJ software.

Scanning electron microscopy (SEM)

Skin tissue samples were cut into small pieces, fixed in fixative, rinsed with PBS, and postfixed with osmium tetroxide. The samples were then dehydrated through a graded ethanol series, infiltrated and embedded in resin, and polymerized at 60 °C. Ultrathin sections were then cut, stained, and finally observed and imaged via transmission electron microscopy.

ALP expression in diabetic hair follicles

The experiment used 1 g of hair follicle tissue, which was homogenized with 9 mL of physiological saline. After centrifugation at 3000–3500 rpm for 10 min, the supernatant was collected for detection. The samples were clear and free of particles, hemolysis, and bubbles, with approximately 100 μL reserved as a backup. The reagent kit (Biobase Biodustry, CHN) includes R1 and R2, which should be mixed or used separately according to the instructions. The reagents were stored at 2–8 °C. The experiment is performed on the Boco automatic biochemical analyzer, where the parameters are set, and the instrument automatically completes the process after loading the reagents and samples.

Histological assay
On the 14th day following surgery, the animals were sacrificed, and wound tissue and liver samples were collected and processed into paraffin-embedded sections for histological examination. The tissues were initially fixed in 10% formalin and then embedded in paraffin blocks. Sections were cut at a thickness of 5 μm and stained with hematoxylin and eosin (H&E) for observation under a light microscope. Epidermal thickness was measured via ImageJ software. To assess collagen deposition, Masson's trichrome staining was applied, and the collagen-rich area density was quantified via ImageJ.

Ki67 immunofluorescence
To distinguish endogenous wound tissue proliferation from proliferation within transplanted hair follicles, Ki67 expression was evaluated specifically in the wound bed, which is composed of regenerated dermis and epidermis, and Ki67 immunofluorescence staining was performed on the wound tissue sections on day 14. After deparaffinization, rehydration, antigen retrieval, and blocking, the sections were incubated with a rabbit anti-Ki67 primary antibody (1:200, Servicebio, CHN, NO.[GB121141]), followed by a goat anti-rabbit secondary antibody (1:500, Seracare, USA, NO.[5220–0336]), and counterstained with DAPI. Images were captured at 20× magnification via a fluorescence microscope, with five randomly selected fields per sample analyzed. The percentage of Ki67-positive cells in each group was quantified via Image-Pro Plus software.

CD31 and VEGF immunohistochemistry and quantification of microvessel density
To evaluate angiogenesis after treatment, CD31 and VEGF immunohistochemistry was performed on wound tissue sections on day 14 with a rabbit anti-rat CD31 antibody (1:200, Abcam, UK, NO. [ab182981])/rabbit anti-rat VEGF antibody (1:200, BOSDE, CHN, NO. [BA0407]). After deparaffinization and rehydration, the sections were subjected to antigen retrieval via microwave heating, treated with 3% hydrogen peroxide, and blocked with 5% goat serum. The sections were then incubated overnight at 4 °C with the primary antibody, followed by a 1-hour incubation with an HRP-conjugated goat anti-rabbit secondary antibody (1:500, Seracare, USA, NO. [5220 – 0336]), and visualized via a DAB kit (ZSGB-BIO, China). The slides were counterstained with hematoxylin and observed under a fluorescence microscope (Nikon, JPN). For analysis, the three regions with the most prominent neovascularization at 5× magnification were selected from each slide, and three random fields per region were imaged at 20× magnification. Microvessel density (MVD) was calculated via Image-Pro Plus software as the average number of vessels per image.

Elisa
The skin tissue samples were minced, homogenized, and centrifuged to collect the supernatant for analysis. In accordance with the instructions of the ELISA kit (Ruixinbio, CHN), standard solutions and samples were added to ELISA plates precoated with specific antibodies (Ruixinbio, CHN), followed by incubation, washing, and the addition of HRP-conjugated secondary antibodies (Ruixinbio, CHN) and substrate for color development. The reaction was terminated with a stop solution, and the absorbance was measured at 450 nm via a microplate reader. The concentrations of IL-6 (Ruixinbio, CHN, No. [RX203049M]), IL-1β (Ruixinbio, CHN, No. [RX203063M]), and TNF-α (Ruixinbio, CHN, No. [RX202412M]) in the samples were calculated on the basis of the standard curve and statistically analyzed.

Statistical analysis
All the statistical analyses were performed via GraphPad Prism 8.0.1, and the data are presented as the mean ± standard deviation ($\overline{X} \pm SD$). Comparisons between two unpaired groups were conducted via independent samples t tests. For comparisons among multiple groups, one-way or two-way analysis of variance (ANOVA) was applied, followed by Bonferroni post hoc correction. A p value of < 0.05 was considered statistically significant.

DISCUSSION

Wound healing is a complex and highly orchestrated biological process that is essential for maintaining skin barrier function[27]. However, diabetic ulcers, as one of the most common and severe complications in patients with diabetes, have emerged as a major global public health issue. They impose a significant economic burden on patients and severely impair their quality of life. In individuals with diabetes, hyperglycemic conditions lead to dysfunction of epidermal and endothelial cells, persistent inflammatory responses, and diffuse, multifocal vascular lesions, all of which markedly impair the wound healing process[28–29]. Clinically, such healing impairments are most frequently observed in patients with type 2 diabetes mellitus (T2DM) and, if left untreated, can progress to diabetic foot ulcers or even limb amputation, posing serious threats to patient survival[28].

Although conventional therapies offer some benefit, their overall efficacy remains limited. In recent years, advances in regenerative medicine have identified hair follicles and their associated stem cells as promising candidates in the field of wound repair. Human hair follicle stem cells (HFSCs) are advantageous because of their widespread distribution, abundance, ease of isolation, minimal damage to the donor site, rapid regeneration cycle, and ability to be harvested repeatedly regardless of donor age. Moreover, HFSCs serve as robust stem cell reservoirs that play critical roles in both chronic diabetic wound healing and tissue engineering. Compared with mesenchymal stem cells (MSCs), which are currently utilized in the treatment of chronic diabetic wounds, HFSCs exhibit superior regenerative capacity, greater survival and functional stability, and lower immunogenicity. In diabetic mouse models, HFSCs demonstrated increased therapeutic efficacy in wound repair and improved posthealing skin quality[30–31]. Consistent with the findings of Qiu et al.[32], HFSC transplantation increased collagen fiber deposition and remodeling in the wound bed, contributing to the formation of skin tissue with an architecture more closely resembling that of normal skin. This not only enhances healing quality but also reduces scar formation.

To better replicate the diabetic mouse model, we employed a protocol of low-dose, continuous intraperitoneal streptozotocin (STZ) injections. Prior to establishing the wound model, we carefully monitored the physiological status of each mouse to ensure sustained hyperglycemia. Only when blood glucose levels remained elevated for four weeks did we proceed, thereby ensuring prolonged hyperglycemia-induced endothelial dysfunction and microcirculatory impairment. After four weeks, we compared microcirculatory alterations, liver histopathology (HE staining), and alkaline phosphatase (ALP) expression in hair follicles between STZ-induced diabetic mice and controls. Our screening revealed that not all the mice maintained stable hyperglycemia after STZ administration; only approximately 60% exhibited sustained blood glucose levels exceeding 16.7 mmol/L. In these mice, transmission electron microscopy revealed significant microvascular abnormalities, including localized and full-thickness basement membrane thickening in the dorsal skin, indicating microcirculatory dysfunction. Additionally, HE-stained liver sections from the high-fat, high-glucose (HG) group presented disorganized hepatic cords, hepatocyte hypertrophy, cytoplasmic lipid vacuoles, and numerous lipid droplets, reflecting features of hyperlipidemia and fatty liver—pathological hallmarks also observed in T2DM patients.

Furthermore, we observed marked suppression of hair follicle activity in diabetic mice, likely due to disruption of the specialized microenvironment surrounding HFSCs, particularly in the dermal papilla. Diabetes-induced local ischemia and hypoxia in this region may further impair follicular function. Studies have reported that a glucose concentration of 30 mM destabilizes HIF-1α, delays wound healing by exacerbating oxidative stress, and inhibits HFSC activation[33]. Moreover, hyperglycemia suppresses the Wnt/β-catenin signaling pathway, downregulating genes such as Lgr4, Lgr5, Wnt4, and Wnt8a, ultimately hindering Lgr5 + HFSC activation, follicular regeneration, and epidermal cell proliferation[34]. These mechanisms may contribute to the impaired skin turnover and chronic wound formation frequently observed in diabetic patients[35–36].

Emerging evidence supports the use of local hair follicle transplantation as an effective strategy for chronic ulcer repair, suggesting that this approach may also hold promise for the treatment of diabetic wounds[8]. In recent years, with the deepening understanding of skin appendages, hair follicles have garnered widespread attention because they are the largest reservoir of stem cells within the skin[37–40]. Hair follicle stem cells (HFSCs) are believed to possess multipotent differentiation potential and hold great promise for applications in regenerative medicine[41]. However, the specific mechanisms by which HFSCs exert therapeutic effects during transplantation remain unclear. In this study, we found that hair follicles from both normal and diabetic mice promoted epidermal regeneration by enhancing granulation tissue formation, angiogenesis, and collagen deposition. Moreover, hair follicle transplantation increased epidermal thickness. To our knowledge, this is the first study to report the promoting effect of hair follicle transplantation on wound healing under hyperglycemic conditions.

These results demonstrated that although persistent hyperglycemia in diabetic mice impaired follicular activity, transplantation still accelerated wound repair. Surprisingly, the DW + HF(NG) group exhibited greater wound healing efficiency than did the DW + HF(HG) group and even outperformed the NC + HF(NG) group. These findings suggest that hair follicles from normoglycemic environments have greater intrinsic activity. Additionally, this result implies that hair follicle transplantation may result in unique immune-privileged properties. A moderate increase in blood glucose levels may activate exogenous follicles, thereby increasing their contribution to wound repair, which aligns with previous studies[7]. We speculate that the therapeutic effects of hair follicle transplantation are closely associated with their abundant stem cell populations. Under prolonged hyperglycemic conditions, the blood supply and activity of hair follicles may be impaired; however, upon transplantation, HFSCs may partially recover their activity and become reactivated. These cells can then secrete paracrine factors that recruit and stimulate resident stem cells from adjacent, undamaged tissues to participate in wound healing. One such factor is vascular endothelial growth factor (VEGF), which promotes microcirculatory formation.

Previous studies have shown that hair follicles in the anagen phase can effectively enhance wound healing. In C57BL/6 mice, trunk hair follicles are typically in the anagen phase at approximately 10 weeks of age. In the present study, whisker follicles were harvested from 16-week-old mice. Although the growth cycle of mouse whisker follicles has not been extensively characterized, some studies suggest that the duration of the anagen phase determines hair length. For example, human scalp hair follicles remain in anagen for approximately 2–8 years, whereas eyelashes remain in this phase for only 2–3 months. It is therefore plausible that whisker follicles may have a longer anagen phase than trunk follicles in mice[42]. Nonetheless, the relatively lower healing efficiency observed following transplantation of high-glucose follicles in this study may also be attributed to the follicles being in a nonanagen phase at the time of harvesting, which warrants further investigation.

This study focused on the analysis of wound healing in mice within a 14-day period and did not investigate long-term tissue remodeling, scar formation, or functional restoration. However, previous studies have conducted hair follicle (HF) transplantation into scar tissue over a six-month period and reported that anagen-phase HFs can attenuate fibrotic phenotypes through paracrine signaling by releasing remodeling factors such as VEGF and EGF. These findings offer new insights into the development of regenerative strategies for remodeling mature scars[43]. Not surprisingly, adequate microcirculation appears to be closely associated with improved wound healing outcomes[20]. In our study, HF transplantation increased the number of CD31-positive vessels within the wound tissue of diabetic mice, suggesting enhanced angiogenesis. VEGF, a key angiogenic factor, promotes endothelial cell mitosis, inhibits apoptosis, increases vascular permeability, and facilitates cell migration, all of which contribute to the regulation of angiogenesis[22]. The Ki67 immunofluorescence results in our study indicated that HF transplantation effectively accelerated wound closure and promoted both cell proliferation and angiogenesis within granulation tissue in both normal and diabetic mice. Compared with that in nondiabetic wounds, wound healing in diabetic mice is delayed, primarily due to a prolonged inflammatory phase[8]. One of the key factors contributing to persistent inflammation in diabetic ulcers is the impaired transition of macrophages from the proinflammatory M1 phenotype to the anti-inflammatory M2 phenotype[44]. M1 macrophages secrete a range of proinflammatory cytokines, such as TNF-α, IL-1β, and IL-6, which exacerbate

tissue damage, whereas M2 macrophages release anti-inflammatory cytokines, such as IL-10 and TGF-β1, which help suppress inflammation.

Another crucial benefit of HF transplantation lies in its notable anti-inflammatory properties. In this study, HF transplantation downregulated the expression of inflammatory cytokines—including TNF-α, IL-6, and IL-1β—in the wound tissue of diabetic mice, thereby mitigating inflammation and reducing vascular endothelial damage. Interestingly, this anti-inflammatory effect was less pronounced in wounds from nondiabetic mice, suggesting that the immunomodulatory capacity of mesenchymal stem cells (MSCs) within HFs may play a key role in this context[31].

In summary, this study demonstrated that hair follicle (HF) transplantation effectively accelerates wound healing in diabetic mice by promoting re-epithelialization, wound contraction, angiogenesis, and collagen deposition while simultaneously reducing the inflammatory response. HF transplantation not only provides a robust source of stem cells but also results in unique immune-privileged properties. Therefore, HF transplantation represents a promising therapeutic strategy for the treatment of diabetic wounds. However, the current findings remain at the preclinical stage, and further investigations are needed to elucidate the underlying molecular mechanisms, evaluate long-term efficacy, and assess the feasibility and safety of clinical translation.

As we aim to publish this study in the near future, it is important to acknowledge its limitations. First, we used only male mice in this study; future research will include female mice to account for potential sex-related differences. Second, the study duration was relatively short, and we focused only on wound changes within two weeks posttransplantation, without evaluating long-term tissue remodeling, scar formation, or functional recovery. Third, we did not further isolate HF-derived stem cells or secreted factors to determine their specific contribution to wound repair, which warrants further experimental exploration. Finally, while this study demonstrated the beneficial effects and partial mechanisms of HF transplantation on diabetic wound healing, many aspects remain unclear. We plan to expand the dataset and conduct additional studies to further clarify these mechanisms in the future.

Conclusion

1. Hair follicles can promote wound healing in diabetic mice under both hyperglycemic and normoglycemic conditions, with syngeneic transplantation resulting in increased repair efficiency in a normoglycemic environment.
2. Hyperglycemia not only induces microcirculatory disturbances but also suppresses hair follicle activity.
3. Following transplantation, hair follicles facilitate diabetic wound healing by secreting vascular endothelial growth factor (VEGF), increasing microvessel density, accelerating granulation tissue formation, inhibiting proinflammatory cytokine expression, and alleviating wound inflammation.

Data availability

The datasets generated during and/or analysed during the current study are available. The data are presented in supplementary materials. The raw data supporting the conclusions of this article will be made available by the authors (Qian Hu) on request.

Received: 26 December 2024; Accepted: 17 July 2025
Published online: 13 August 2025

References

1. Armstrong, D. G., Tan, T. W., Boulton, A. J. M. & Bus, S. A. Diabetic foot ulcers: a review. *JAMA* **330** (1), 62–75. https://doi.org/10.1001/jama.2023.10578 (2023).
2. Meza-Torres, B. et al. Adherence to general diabetes and foot care processes, with prompt referral, are associated with amputation-free survival in people with type 2 diabetes and foot ulcers: a scottish national registry analysis. *journal of diabetes research* https://doi.org/10.1155/2022/7414258 (2022).
3. Davis, F. M. et al. Dysfunctional wound healing in diabetic foot ulcers: new crossroads. *Curr. Diab Rep.* **18** (1), 2. https://doi.org/10.1007/s11892-018-0970-z (2018).
4. Jimenez, F., Alam, M. & Vogel, J. E. Hair transplantation: basic overview[J]. *J. Am. Acad. Dermatol.* **85**, 803–814. https://doi.org/10.1016/j.jaad.2021.03.124 (2021).
5. Nuutila, K. Hair follicle transplantation for wound repair. *Adv. Wound Care (New Rochelle).* **10** (3), 153–163. https://doi.org/10.1089/wound.2019.1139 (2021).
6. Lough, D. M. et al. Transplantation of the LGR6 + epithelial stem cell into full-thickness cutaneous wounds results in enhanced healing, nascent hair follicle development, and augmentation of angiogenic analytes. *Plast. Reconstr. Surg.* **133** (3), 579–590. https://doi.org/10.1097/PRS.0000000000000075 (2014).
7. Wang, M. et al. Diabetes mellitus inhibits hair follicle regeneration by inducing macrophage Reprogramming-Mediated pyroptosis. *J. Inflamm. Res.* **17**, 6781–6796. https://doi.org/10.2147/JIR.S469239 (2024).
8. Saha, D. et al. Hair follicle grafting therapy promotes re-emergence of critical skin components in chronic nonhealing wounds. *JID Innov.* **1** (3), 100041. https://doi.org/10.1016/j.xjidi.2021.100041 (2021). Published 2021 Jul 9.
9. Martínez, M. L. et al. Hair follicle-containing punch grafts accelerate chronic ulcer healing: a randomized controlled trial. *J. Am. Acad. Dermatol.* **75** (5), 1007–1014. https://doi.org/10.1016/j.jaad.2016.02.1161 (2016).
10. Jiménez, F. et al. A pilot clinical study of hair grafting in chronic leg ulcers. *Wound Repair. Regen.* **20** (6), 806–814. https://doi.org/10.1111/j.1524-475X.2012.00846.x (2012).
11. Serra, R. et al. Skin grafting for the treatment of chronic leg ulcers - a systematic review in evidence-based medicine. *Int. Wound J.* **14** (1), 149–157. https://doi.org/10.1111/iwj.12575 (2017).
12. Martínez Martínez, M. L., Escario Travesedo, E. & Jiménez Acosta, F. Hair-follicle transplant into chronic ulcers: a new graft concept. Trasplante de folículos Pilosos En úlceras crónicas: Un Nuevo Concepto de Injerto. *Actas Dermosifiliogr.* **108** (6), 524–531. https://doi.org/10.1016/j.ad.2017.02.013 (2017).
13. Jansen, T. M. et al. Hair follicle punch grafts in hard-to-heal wounds: A monocenter study and patient survey. *Health Sci. Rep.* **7** (8), e2319. https://doi.org/10.1002/hsr2.2319 (2024).

14. Ansell, D. M. et al. MJ. Exploring the hair growth-wound healing connection: anagen phase promotes wound re-epithelialization. *J. Invest. Dermatol.* **131** (2), 518–528. https://doi.org/10.1038/jid.2010.291 (2011).
15. Rippa, A. L., Kalabusheva, E. P. & Vorotelyak, E. A. Regeneration of dermis: scarring and cells involved. *Cells* **8** (6), 607. https://doi.org/10.3390/cells8060607 (2019). Published 2019 Jun 18.
16. Miranda, J. J. et al. Hair follicle characteristics as early marker of type 2 diabetes. *Med. Hypotheses*. **95**, 39–44. https://doi.org/10.1016/j.mehy.2016.08.009 (2016).
17. Gan, Y. Y. et al. Theoretical basis and clinical practice for FUE megasession hair transplantation in the treatment of large area androgenic alopecia. *J. Cosmet. Dermatol.* **20** (1), 210–217. https://doi.org/10.1111/jocd.13432 (2021).
18. Kwack, M. H. et al. Overexpression of alkaline, Overexpression of alkaline phosphatase improves the hair-inductive capacity of cultured human dermal papilla spheres. *J Dermatol Sci.* https://doi.org/10.1016/j.jdermsci.2019.07.008 (2019).
19. Jonat, W. & Arnold, N. Is the Ki-67 labelling index ready for clinical use? *Ann. Oncol.* **22** (3), 500–502. https://doi.org/10.1093/annonc/mdq732 (2011).
20. Lowry, D. et al. The difference between the healing and the nonhealing diabetic foot ulcer: a review of the role of the microcirculation. *J. Diabetes Sci. Technol.* **11** (5), 914–923. https://doi.org/10.1177/1932296816658054 (2017).
21. Okonkwo, U. A. & DiPietro, L. A. Diabetes and wound angiogenesis. *Int. J. Mol. Sci.* **18** (7), 1419. https://doi.org/10.3390/ijms18071419 (2017). Published 2017 Jul 3.
22. Goswami, A. G. et al. An appraisal of vascular endothelial growth factor (VEGF): the dynamic molecule of wound healing and its current clinical applications. *Growth Factors*. **40** (3–4), 73–88. https://doi.org/10.1080/08977194.2022.2074843 (2022).
23. Clyne, A. M. Endothelial response to glucose: dysfunction, metabolism, and transport. *Biochem. Soc. Trans.* **49** (1), 313–325. https://doi.org/10.1042/BST20200611 (2021).
24. Faridvand, Y. et al. Dapagliflozin attenuates high glucose-induced endothelial apoptosis and inflammation through AMPK/SIRT1 activation. *Clin. Exp. Pharmacol. Physiol.* **49** (6), 643–651. https://doi.org/10.1111/1440-1681.13638 (2022).
25. Furman, B. L. Streptozotocin-induced diabetic models in mice and rats. *Curr. Protoc.* **1** (4), e78. https://doi.org/10.1002/cpz1.78 (2021).
26. Maric-Bilkan, C., Flynn, E. R. & Chade, A. R. Microvascular disease precedes the decline in renal function in the streptozotocin-induced diabetic rat. *Am. J. Physiol. Ren. Physiol.* **302** (3), F308–F315. https://doi.org/10.1152/ajprenal.00421.2011 (2012).
27. Jin, R. et al. Three-dimensional Bioprinting of a full-thickness functional skin model using acellular dermal matrix and gelatin methacrylamide Bioink. *Acta Biomater.* **131**, 248–261. https://doi.org/10.1016/j.actbio.2021.07.012 (2021).
28. Mansano Pletsch, A. H. et al. Does sensorimotor training influence neuromuscular responses, balance, and quality of life in diabetics without a history of diabetic distal polyneuropathy? *J. Bodyw. Mov. Ther.* **27**, 148–156. https://doi.org/10.1016/j.jbmt.2021.01.012 (2021).
29. Singer, A. J. & Clark, R. A. Cutaneous wound healing. *N Engl. J. Med.* **341** (10), 738–746. https://doi.org/10.1056/NEJM199909023411006 (1999).
30. Wang, Y. et al. Umbilical cord mesenchymal stem cell-derived apoptotic extracellular vesicles ameliorate cutaneous wound healing in type 2 diabetic mice via macrophage pyroptosis Inhibition. *Stem Cell. Res. Ther.* **14** (1), 257. https://doi.org/10.1186/s13287-023-03490-6 (2023). Published 2023 Sep 19.
31. Yang, H. et al. Hair follicle mesenchymal stem cell Exosomal LncRNA H19 inhibited NLRP3 pyroptosis to promote diabetic mouse skin wound healing. *Aging (Albany NY)*. **15** (3), 791–809. https://doi.org/10.18632/aging.204513 (2023).
32. Qiu, W. et al. Activated hair follicle stem cells and Wnt/β-catenin signaling involve in pathnogenesis of sebaceous neoplasms. *Int. J. Med. Sci.* **11** (10), 1022–1028. https://doi.org/10.7150/ijms.8383 (2014).
33. Las Heras, K. et al. Extracellular vesicles from hair follicle-derived mesenchymal stromal cells: isolation, characterization and therapeutic potential for chronic wound healing. *Stem Cell. Res. Ther.* **13** (1), 147. https://doi.org/10.1186/s13287-022-02824-0 (2022).
34. Wang, M. et al. Type 2 diabetic mellitus inhibits skin renewal through inhibiting WNT-Dependent Lgr5 + Hair follicle stem cell activation in C57BL/6 mice. *J. Diabetes Res.* **2022**, 8938276. https://doi.org/10.1155/2022/8938276 (2022).
35. Sun, P. et al. Autophagy induces hair follicle stem cell activation and hair follicle regeneration by regulating Glycolysis. *Cell. Biosci.* **14** (1), 6. https://doi.org/10.1186/s13578-023-01177-2 (2024). Published 2024 Jan 5.
36. Ryu, Y. C. et al. Wnt/β-catenin signaling activator restores hair regeneration suppressed by diabetes mellitus. *BMB Rep.* **55** (11), 559–564. https://doi.org/10.5483/BMBRep.2022.55.11.081 (2022).
37. Zhang, B. & Chen, T. Local and systemic mechanisms that control the hair follicle stem cell niche. *Nat. Rev. Mol. Cell Biol.* **25** (2), 87–100. https://doi.org/10.1038/s41580-023-00662-3 (2024).
38. Garcin, C. L. et al. Hair follicle Bulge stem cells appear dispensable for the acute phase ofwound re-epithelialization. *Stem Cells*. **34** (5), 1377–1385. https://doi.org/10.1002/stem.2289 (2016).
39. Jaks, V., Kasper, M. & Toftgård, R. The hair follicle-a stem cell zoo. *Exp. Cell. Res.* **316** (8), 1422–1428. https://doi.org/10.1016/j.yexcr.2010.03.014 (2010).
40. Gentile, P. et al. Stem cells from human hair follicles: first mechanical isolation for immediate autologous clinical use in androgenetic alopecia and hair loss. *Stem Cell. Investig.* **4**, 58. https://doi.org/10.21037/sci.2017.06.04 (2017). Published 2017 Jun 27.
41. Squillaro, T., Peluso, G. & Galderisi, U. Clinical trials with mesenchymal stem cells: an update. *Cell. Transplantation Vol.* **25** (5), 829–848. https://doi.org/10.3727/096368915X689622 (2016).
42. Park, A. M., Khan, S. & Rawnsley, J. Hair biology: growth and pigmentation. *Facial Plast. Surg. Clin. North. Am.* **26** (4), 415–424. https://doi.org/10.1016/j.fsc.2018.06.003 (2018).
43. Plotczyk, M. et al. Anagen hair follicles transplanted into mature human scars remodel fibrotic tissue. *NPJ Regen Med.* **8** (1), 1. https://doi.org/10.1038/s41536-022-00270-3 (2023). Published 2023 Jan 6.
44. Louiselle, A. E. et al. Macrophage polarization and diabetic wound healing. *Transl Res.* **236**, 109–116. https://doi.org/10.1016/j.trsl.2021.05.006 (2021).

Acknowledgements

Z.L. discloses support for the research of this work from the Guizhou Science Fund Project of the National Natural Science Foundation of China, grant number [82060352,82460450]and [QKHJC-ZK[2025]-469].

Author contributions

Author Contributions• [Q.H.] and [X.P.]: Conceived and designed the study, developed the research framework, and coordinated the overall research efforts, including experimental design and data analysis. processed raw data, and created all visual representations, including figures, graphs, and supplementary materials. Revised the initial draft extensively and confirmed the final manuscript for submission.• [Q.H.], [X.P.], and [Y.Y.]: Drafted the initial manuscript, covering the introduction, methods, results, and discussion sections. Integrated feedback from all co-authors during the writing and revision stages. Managed reference formatting and ensured adherence to journal submission guidelines.• [L.Z.]: Supervised all stages of the study, Provided critical guidance on experimental design, data interpretation, and manuscript structure. Reviewed the manu-

script at each stage to ensure quality and coherence. Provided essential resources, including clinical samples, specialized equipment, and proprietary algorithms. Contributed to the study design through technical guidance and strategic input.All authors reviewed the manuscript critically for intellectual content, provided constructive feedback during its preparation, and approved the final version for submission.

Declarations

Competing interests

The authors declare no competing interests.

Additional information

Supplementary Information The online version contains supplementary material available at https://doi.org/10.1038/s41598-025-12564-9.

Correspondence and requests for materials should be addressed to Z.L.

Reprints and permissions information is available at www.nature.com/reprints.

Publisher's note Springer Nature remains neutral with regard to jurisdictional claims in published maps and institutional affiliations.